

THE INITIAL ANALYSIS OF THE AERODYNAMIC CHARACTERISTICS OF A 3D PRINTED MODEL OF AN AIRCRAFT

Tomasz Lusiak

*Lublin University of Technology
Faculty of Mechanical Engineering, Department of Thermodynamics
Fluid Mechanics and Aviation Propulsion Systems
Nadbystrzycka Street 36, 20-618 Lublin, Poland
tel.: +48 81 538 42 84, fax: +48 81 538 47 49
e-mail: t.lusiak@pollub.pl*

Robert Babel

*Polish Air Force Academy
Aeronautics Faculty, Department of Airframe and Engine
Dywizjonu 303 Street 35, 08-521 Deblin, Poland
tel.: +48 261 517 430, fax: +48 261 517 417
e-mail: r.babel@wsosp.pl*

Abstract

The aerodynamic research into models of an aircraft aims at creating the main characteristics of aerodynamic forces and moments and the aerodynamic characteristics of coefficients of aerodynamic forces and moments, based on real dimensions. The method of 3D printing was used to create a model of an aircraft. The model with the previously set printing parameters and commands for a 3D printer, in the right order, was imported into MakerBot Print. The final stage was printing the model. The printed components of the model of an aircraft were imperfect due to the incorrectly set printing parameters. The model with the previously set printing parameters and commands for a 3D printer, in the right order, was imported into MakerBot Print. The final stage was printing the model. The printed components of the model of an aircraft were imperfect due to the incorrectly set printing parameters. The printing parameters were corrected in the next printing sessions so the surfaces of the components were good enough and grinding was unnecessary. Some excess material was removed in each of the printed components, and the slots were cleaned. Then, the individual models were put together.

The article describes the technique of creating a model of an aircraft to map its exact geometry for experimental wind tunnel research. 3D printing enables us to experimentally investigate a created geometry, in particular to investigate further prior to releasing an aircraft to service. The 3D model employs the model created in line with the previous CFD analysis.

Keywords: *air transport, simulation, wind tunnel, experimental analysis, gyroplane*

1. Introduction

The behaviour of the aircraft after tripping on the strength turbulence are characterized by these property undisturbed motion of an aircraft which are known under the name of stability and smooth. A prerequisite to this, to the movement of the aircraft was given, is not only a balance between all the forces acting on the aircraft, but also balance moments against the three coordinate axes (x, y, z), passing through its centre of gravity [1].

The balance of the aircraft should be matronly; it means aircraft derived from the State of balance by some external factor, for example. Gust, should in a sufficiently short time return to the United States balance automatically and without the intervention of a remote control (at least when the disturbance is not too large). The concept of stability and balance are so closely related [2].

Speaking of stability assumes the existence of a balance, because otherwise, the concept of stability would be pointless. Statics static aircraft is called its ability to return (without remote controller) to the location of the balance between when to stop working the reasons that this balance of a breach. The stability of dynamic specifies while kind of movements, which performs aircraft returning to the position (e.g., number of, amplitude and time misalignment).

Static and dynamic stability issues are closely and inseparably linked, to the plane was sedate dynamically it must be staid. The stability of the aircraft relative to the y-axis is called the longitudinal stability; provides them tail. Stability relative to the x-axis and z-axis, provided by sheer wings and tail direction is called a lateral and directional. However, considering it as the stability of the side, as they are closely linked use of modified plastics as ablative materials protecting against excessive temperature increase was connected with the middle of the 20TH century, directly with arms industry as well as aeronautical [3].

Airfoil aerodynamic characteristics are determined in specialized theoretical and experimental aerodynamic tunnels through appropriate treatments for the profile of the lobe of an infinite extension, which allows you to convert these characteristics for the lobes of any longer.

In the case at hand, the profile is only friction and profile resistance, without the induced resistance characteristic of a finite span panel. The minimum value of the resistance coefficient shall be at the angle of attack of α_0 , which corresponds to a value of the load-carrying capacity coefficient of zero. The value of this coefficient increases with the thickness of the profile [8].

Characteristics are with the most information about the properties of the profiles. It allows you to calculate the performance of your aircraft. The polar range is limited to a range slightly exceeding α_{kr} . The poles may depending on different flight conditions (e.g. take-off, landing, climb, maximum speed) both because of different Reynolds numbers and because of different positions of different parts of the aircraft. An important factor is also the lifting force acting on the horizontal plane to ensure the balance of longitudinal moments acting on the plane. This force is variable for different angles of attack, flight speed and can be adjusted by tilting the rudder [4].

When K excellence is equal to maximum angle excellence, maximum range is achieved. Maximum perfection is achieved when the optimum angle of attack is reached. This is the parameter that determines the aerodynamic properties of the profile [9, 10].

2. The course of experimental studies

In order to carry out the investigation, we prepared individual elements of the hull model were made in FDM technology of 3D printing.

The FDM (Fused Deposition Modelling) method enables the printing of durable thermoplastic parts. In FDM technology, we have the possibility to build conceptual models and functional prototypes of high quality from materials with specific mechanical properties.

Printers that use FDM technology create parts layer by layer by applying heated thermoplastic material. Prototypes are built of two materials: model and auxiliary – supporting (supports designed to support complex shapes, to preserve the set dimensions). The material is fed through the nozzles and pressed by means of nozzles mounted on the print head, which are designed for several layers of the material to be applied. This allows a choice of layers from 0.127 mm to 0.330 mm. The printing process is followed by the removal of the support material. The models are thrown into a chamber with a water solution and a specially designed detergent. In the chamber, the material is melted under the influence of temperature and after some time the part is ready for use (Fig. 1).

The tests were carried out in a closed-circuit aerodynamic tunnel with an open-circuit circular measuring space. A diagram of the tunnel is shown in the Fig. 2.

A positioning system is installed inside the open measuring area to allow the installation of the model. The research was carried out with the use of multi-component force and torque sensor, so called aerodynamic 6-component balance [6].



Fig. 1. Model parts printed by FDM

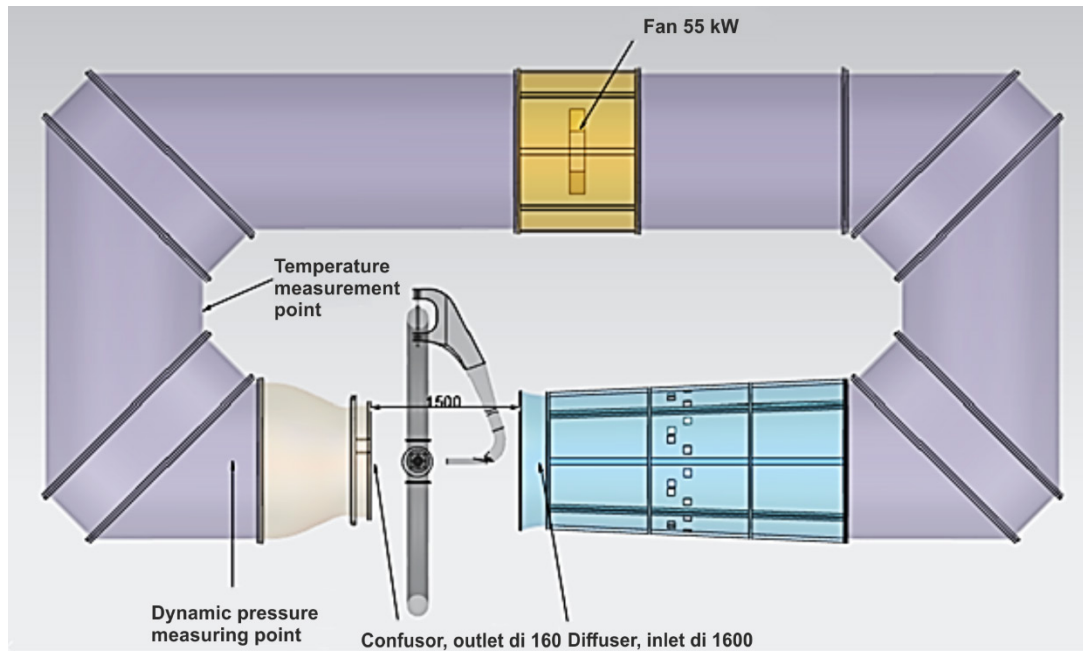


Fig. 2. Diagram of the tunnel; counter-clockwise air circulation [5]

The centre of gravity (the reference point of the measured forces) is located at the centre of rotation of the positioning system. The measuring system works in the automatic mode by loading the model positions based on the prepared grid of angles. The measurement is the result of recording the value of the determined mean with the measurement of the stationarity of the result.

Dimensions of measuring space: $D=\varnothing 1.2 \text{ m}$, $L=1.5 \text{ m}$,
 Dimension of inlet PP to the axis of the: $l=0.443 \text{ m}$,
 Air speed: 40 m/s ,
 The ranges of angles: $\alpha \in \langle -30; 25 \rangle$ and $\beta \in \langle -25; 25 \rangle$,
 Measurement of force and moment $F_x=80 \text{ N}$, $F_y=300 \text{ N}$, $F_z=150 \text{ N}$,
 The ranges of weight loads: $M_x=5 \text{ Nm}$, $M_y=15 \text{ Nm}$, $M_z=7 \text{ Nm}$.

The forces and moments referred to the components in the following section are also indicated in the diagram of the coordinate system. The dimensions given in the Tab. 1 are used to dimension the forces and moments to the corresponding coefficients [7].

The measurement was made in a coordinate system related to the model (*body*) $F_b = [T \ C \ N]$, rotation matrices with angles (α, β) as shown (Fig. 3) were used for the transition to the reference system related to the speed vector (*wind*) $F_w = [D \ S \ L]$.

The results were presented in a system of coordinates of slip angles and attack angle. The convention of presenting the results of the angle of divergence function shall also be applied in aviation practice. It is usually assumed that the angles of β and Ψ slip are linked by a relationship:

$$\sin\beta = -\sin\Psi.$$

The research was carried out in geometrical configurations, which is listed in Tab. 2.

Tab. 1. The dimensions of the characteristic mode

	Real object	Model
r	5m	$0.625m^3$
$A = \pi r^2$	$78.5398m^2$	$1.22718m^2$
$A r = \pi r^3$	$392.699m^3$	$0.766999m^3$

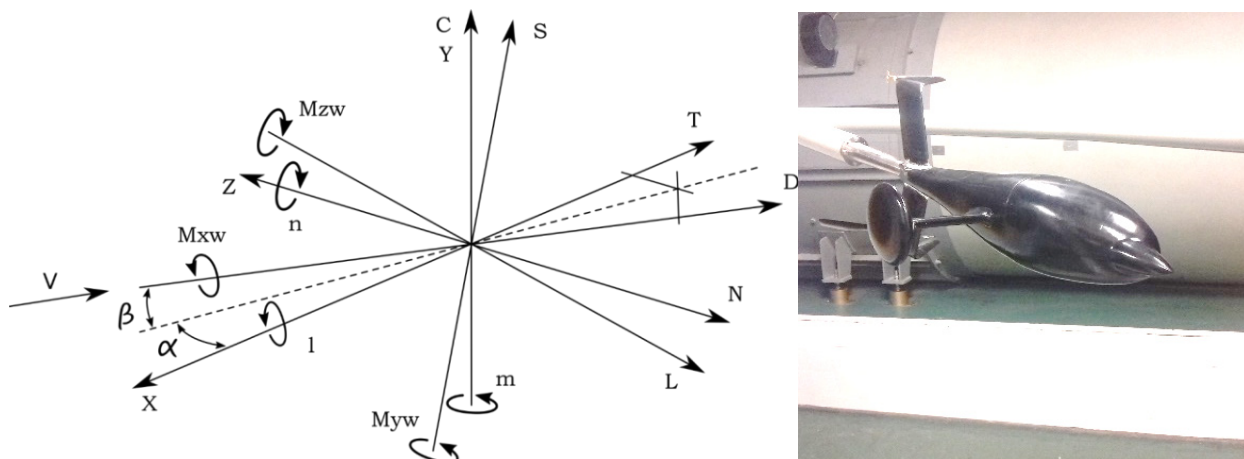


Fig. 3. Adopted coordinate system and photo model in tunnel

Tab. 2. Design table research

Item	Gyroplane configuration	Angle of attack α [steps]	Attention
1	Gyroplane complete-chassis hidden	od -20 do +20 co 4	Basic characteristics

3. Test results

The measurement series listed in the table were carried out in the previously established positions of the model using the so-called grid of points in the angular space. The main parameters of the evaluation showed in Tab. 3.

A comparison of the tilting and tilting air resistance characteristics, for both chassis less and chassis-based systems, shows a slightly higher resistance of the chassis-based system, with the difference increasing with tilting and tilting. This can be caused by turbulence behind the windscreens of the chassis.

As can be seen from the graph below, the resistance force for the chassis system is higher for all the attack angles tested (Fig. 4).

Tab. 3. Test result of research

Alfa	Beta	Fz	My	Fx	Fy	Mz	Mx	Cx	Cz	Cz/Cx	Cmx	Cmy	Cmz	
-20	0	-10.0854	2.20976	5.788513	-0.41	-0.02697	-0.03053	0.012118	-0.02111	-1.74232	-0.0001	0.007401	-0.00009	-0.00086
-16	0	-9.40819	2.160332	4.811643	-0.325	-0.01924	-0.02629	0.010078	-0.01971	-1.9553	-8.8E-05	0.00724	-6.4E-05	-0.00068
-12	0	-8.4785	2.051877	3.649529	-0.356	0.011994	-0.04054	0.007605	-0.01767	-2.32318	-0.00014	0.006842	0.00004	-0.00074
-8	0	-6.30882	1.560623	2.677071	-0.238	-0.02438	-0.03105	0.005572	-0.01313	-2.35661	-0.0001	0.005197	-8.1E-05	-0.0005
-4	0	-3.40773	0.900387	2.230144	-0.202	-0.03048	-0.02323	0.004629	-0.00707	-1.52803	-7.7E-05	0.00299	-0.0001	-0.00042
-2	0	-1.76733	0.498823	2.055931	-0.108	-0.04774	-0.01685	0.004262	-0.00366	-0.85962	-5.6E-05	0.001655	-0.00016	-0.00022
0	0	-0.015	0.074284	1.934	-0.07	-0.0583	-0.02057	0.004004	-3.1E-05	-0.00776	-6.8E-05	0.000246	-0.00019	-0.00015
2	0	1.537136	-0.31821	1.856776	-0.056	-0.06314	-0.02107	0.003846	0.003184	0.827852	-0.00007	-0.00106	-0.00021	-0.00012
4	0	3.166573	-0.74562	1.808294	-0.069	-0.06083	-0.02482	0.003745	0.006558	1.751139	-8.2E-05	-0.00247	-0.0002	-0.00014
8	0	6.07789	-1.50611	1.934707	-0.003	-0.08191	-0.03994	0.004003	0.012574	3.141504	-0.00013	-0.00499	-0.00027	-6E-06
12	0	8.447318	-2.06213	2.492769	0.165	-0.12234	-0.05523	0.005182	0.01756	3.388729	-0.00018	-0.00686	-0.00041	0.000343
16	0	10.27201	-2.57741	3.696549	0.053	-0.13068	-0.12413	0.007692	0.021374	2.778812	-0.00041	-0.00858	-0.00044	0.00011
20	0	10.90388	-2.69753	4.732768	0.1	-0.10423	-0.12296	0.009836	0.022661	2.303912	-0.00041	-0.00897	-0.00035	0.000208

The load bearing capacity of both systems is very similar. The clearest equator is for rake angles above 15° , in which case the chassis system shall be in the lead (Fig. 5).

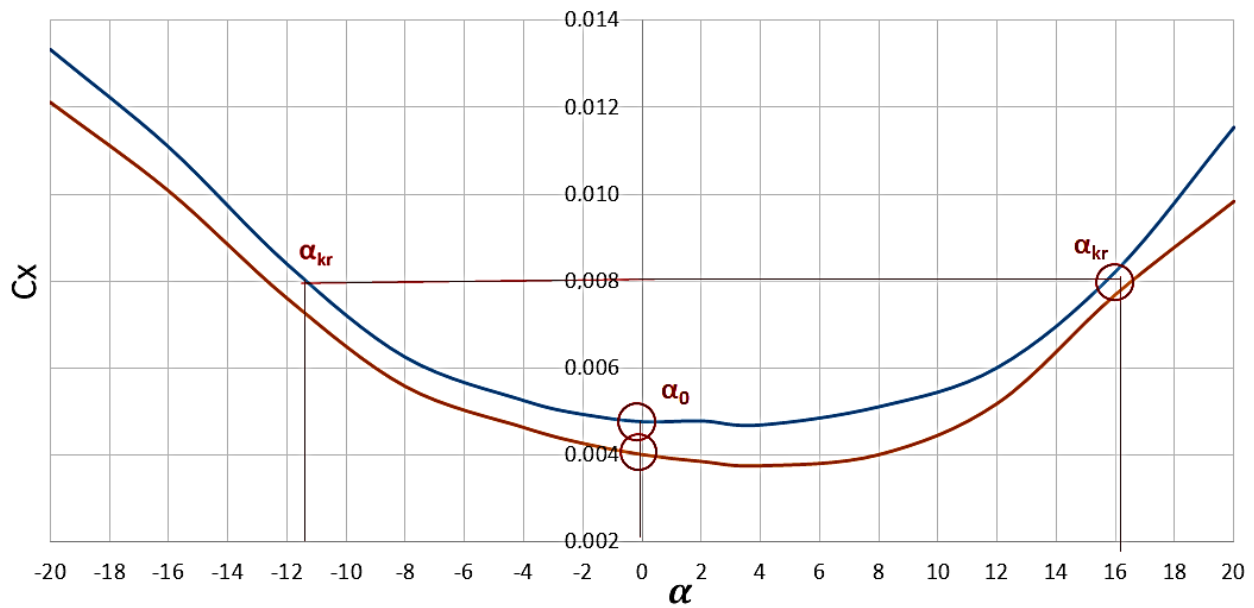


Fig. 4. Characteristics $C_x=f(\alpha)$ (— with aeroplane landing gear, — without aeroplane landing gear)

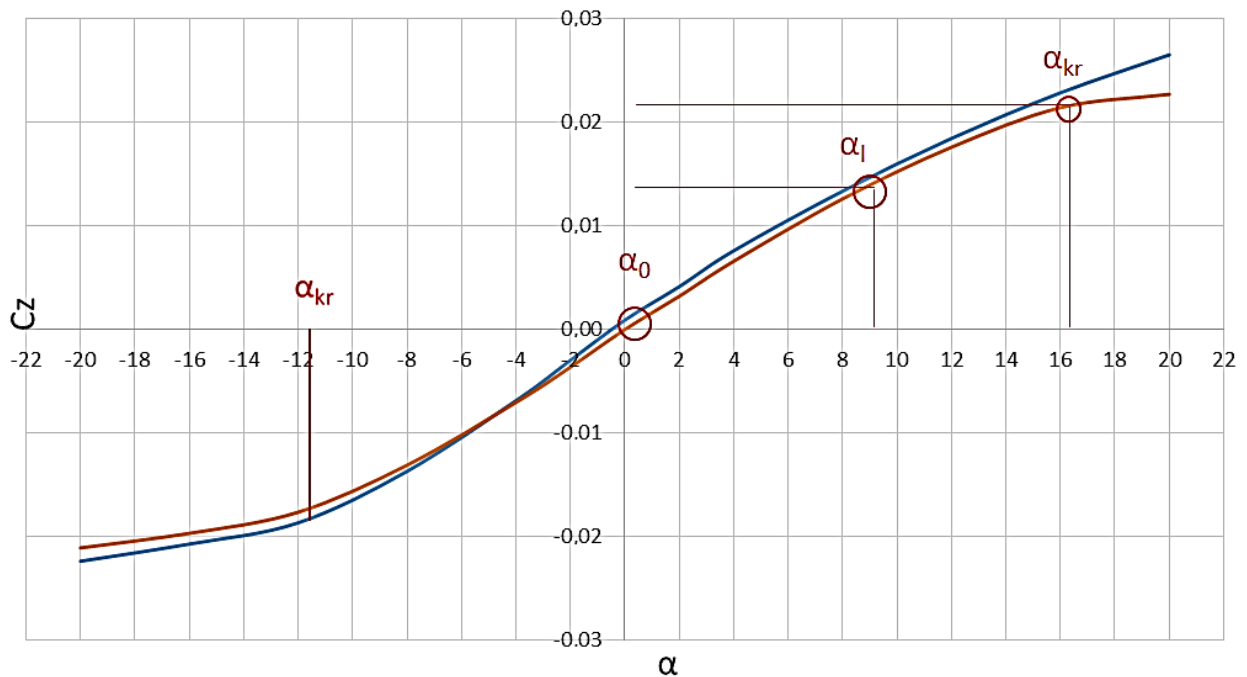


Fig. 5. Characteristics $C_z=f(\alpha)$ (— with aeroplane landing gear, — without aeroplane landing gear)

The aerodynamic excellence, which is the property that best illustrates the efficiency of the structure, shows that the chassis has little influence on it for negative attack angles. For positive rake angles, especially in the range of 5° to 15° , perfection is lower for the chassis less system, i.e. for these rake angles the air resistance created by the carriage is greater than its lifting force (Fig. 6).

The torque along the z-axis shall be the same for all approach angles at zero slip angle. However, reading the chart below we can conclude that the model is asymmetrical or that its installation is inaccurate. It is worth noting that these are very small values of M_z (Fig. 7).

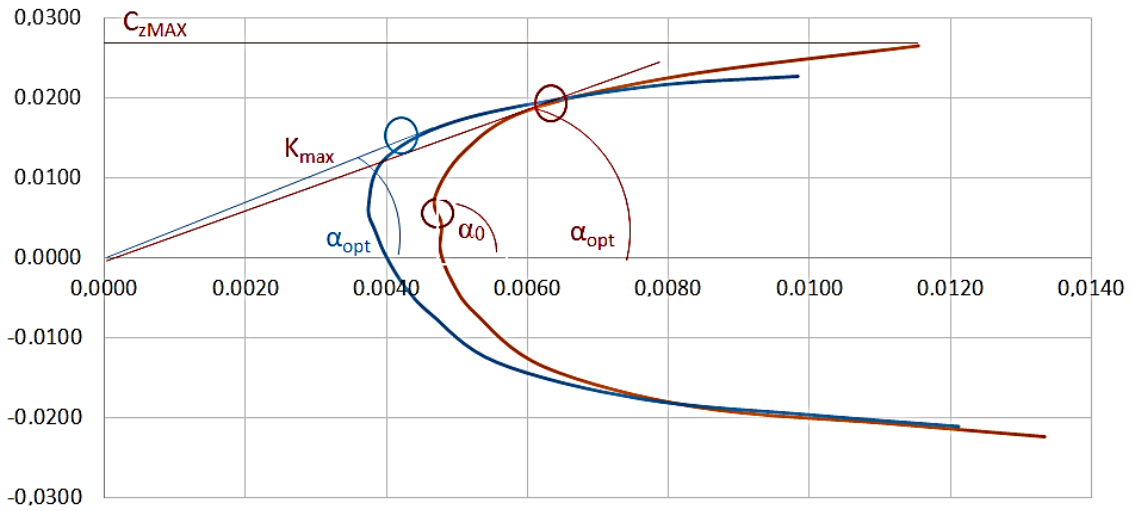


Fig. 6. Characteristics $C_z/C_x = f(\alpha)$ (— without aeroplane landing gear, — with aeroplane landing gear)

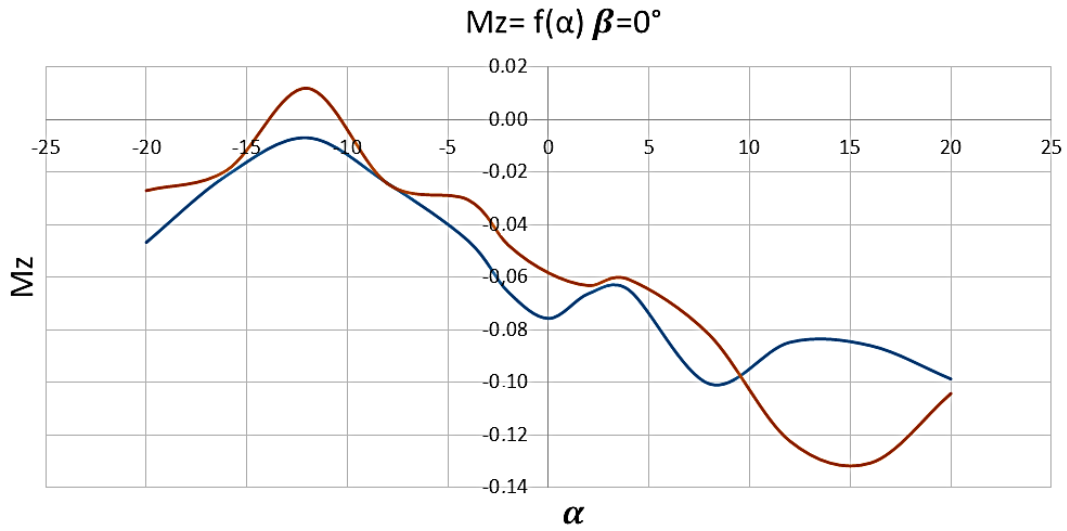


Fig. 7. Characteristics $C_x = f(\alpha)$ (— with aeroplane landing gear, — without aeroplane landing gear)

The torque along the x-axis, or longitudinal axis, shall also be constant for all angles of attack, as in M_x (Fig. 8).

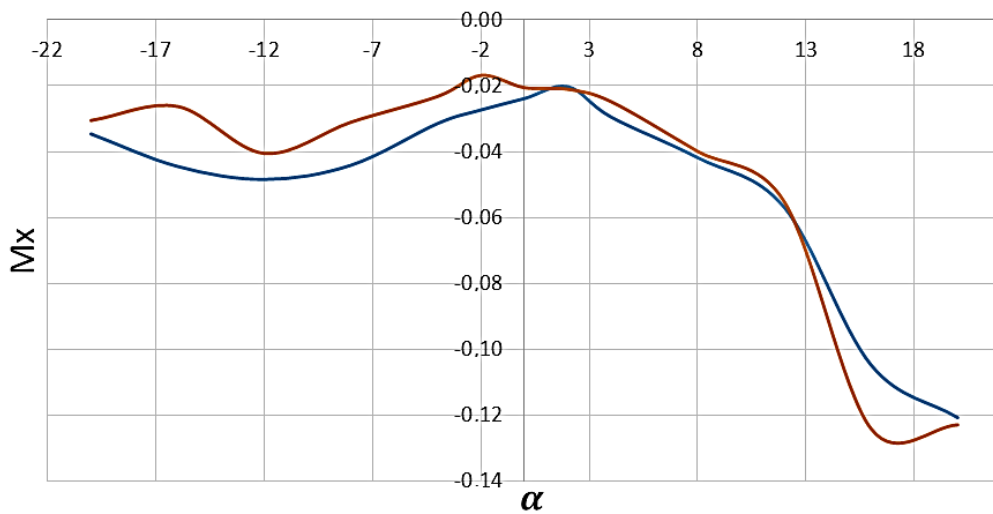


Fig. 8. Characteristics $M_x = f(\alpha)$ (— with aeroplane landing gear, — without aeroplane landing gear)

The torque along the transverse axis, depending on its sign, tilts the model up or down. It is advantageous to keep the momentum as low as possible for the angles of attack corresponding to the horizontal flight (Fig. 9). This means that the chassis system is better in this respect.

The presented results constitute only a small part of the research that should be carried out in the process of constructing a new windmill hull. The results obtained allow only for a preliminary analysis of the impact of changes leading to the optimisation of the structure. In order to thoroughly investigate the problem, much more research should be done and the above relationships should be analysed in other geometrical configurations of the windmill model.

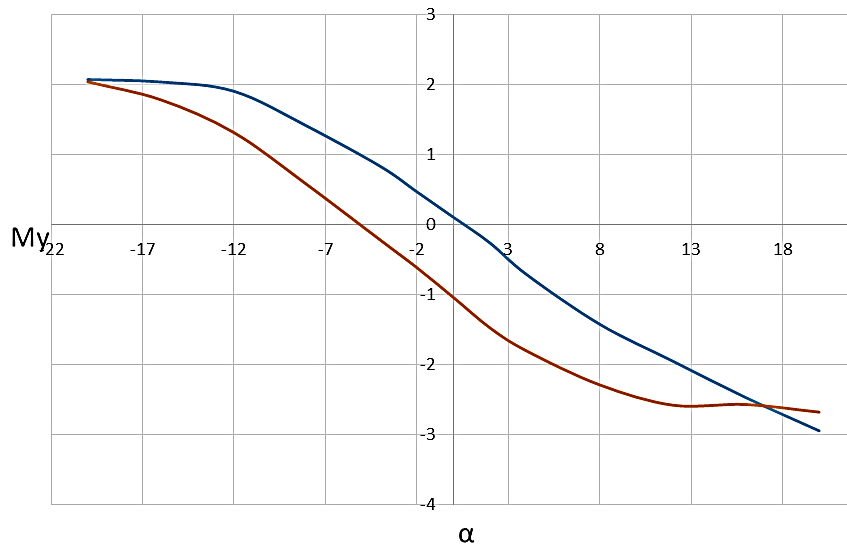


Fig. 9. Characteristics $My = f(\alpha)$ (— with aeroplane landing gear, — without aeroplane landing gear)

3. Conclusion

Research on the model in an aerodynamic tunnel allowed developing characteristics that illustrate its properties. Characteristics have been created for all combinations of slide angle ($-25-25^\circ$) and rake angle ($-20-20^\circ$) for the model with and without chassis. On this basis it can be concluded that the chassis has been very well designed, despite the fact that it increases C_x and reduces C_z and slightly perfection for most of the rake angles and small angles of slip, it should be noted that these are insignificant changes, additionally for large angles of slip the influence of the chassis improves some parameters. If the carriage has a positive influence on the extreme angles of attack and slip, it causes a shift in critical values and an increase in safety.

During the experiments, the windmill model was also tested for tilting moment at various slide angles. The results showed that the aircraft behaved similarly in all configurations, regardless of the value of the slip angle. The characteristics are linear positive over the entire measuring range. As the angle of attack increases, the value of the aerodynamic tilting moment coefficient increases.

As the angle of attack increases, the aerodynamic transverse force coefficient increases. The angle of attack shall be sharply reduced between 12 and 20° . This is a sign of instability. The angle of slip significantly influences the characteristics of the flow of the windmill model without a collision. Depending on the value of the slip angle sign, the value of the attack angle shall be significantly below zero or significantly above zero relative to the vertical axis of the coordinate system.

References

- [1] Czyż, Z., Łusiak, T., Magryta, P., *CFD Numerical Testing for the Effect of Fault on the Aerodynamic Characteristics of Windmills*, Transactions of the Institute of Aviation, 232 pp. 3-14, 2013.

- [2] Łusiak, T., Czyż, Z., Kłoda, Ł., Chabros, M., Dżaman, E., *Comparative analysis of the results of numerical tests of wind turbines with the results of tests in wind tunnels*, 2013.
- [3] Łusiak, T., Wendeker, M., *Aerodynamic research of the Fusincopter hull*, Lublin University of Technology, Department of Thermodynamics, Fluid and Aviation Propulsion Systems, 2/92/NN/2013, Lublin 2013.
- [4] Ruchała, P., Stryczniewicz, W., Czyż, Z., Łusiak, T., *Aerodynamic characteristics of windmill hull for different angles of horizontal impact wedging*, Transactions of the Institute of Aviation, No. 4 (241), pp. 96-107, Warszawa 2015.
- [5] Compa, T., *Aircraft Knowledge Base*, WSOSP, Deblin 2012.
- [6] Wiśniowski, W., *Aerodynamic tunnels in Poland in comparison with world tunnels*, Scientific Publishing House of the Institute of Aviation, Warszawa 2016.
- [7] Barlow, J., Rae, W. H., Pope, A., *Low-speed wind tunnel testing*.
- [8] <https://content.sciendo.com>, 06.04.2018.
- [9] Smykła, I., *Selected aerodynamic and flight mechanics issues (flight rules)*, Warszawa 2008.
- [10] Sobieraj, W., *Aerodynamic*, Wojskowa Akademia Techniczna, Warszawa 2014.

Manuscript received 09 July 2018; approved for printing 12 October 2018